

Robust suboptimal output control for a Twin Rotor MIMO System

Sergey A. Vrazevsky¹, Julia V. Chugina^{1,2}, Igor B. Furtat^{1,2}, Artem S. Kremlev¹

¹Department of Control Systems and Industrial Robotics, ²The Laboratory "Control of Complex Systems"

¹ITMO University, ²IPME RAS

St. Petersburg, Russia

Abstract — The main focus of this paper is the research of practical application of robust suboptimal control for the «Twin Rotor multiple input multiple output (MIMO) System». In this work, MIMO system is represented as dynamically related single input single output (SISO) systems. The robust and suboptimal control algorithm is based on the auxiliary loop method for disturbances compensation and suboptimal linear quadratic regulator (LQR) which is applied to the simplified linearized model of the plant. The proposed approach ensures the high quality of the system functioning and reliability in the presence of parametric uncertainties and external disturbances. Obtained result contributes for control of copters with different configurations. It is experimentally tested on the laboratory platform.

Keywords — suboptimal control; robust control; linear quadratic regulator; auxiliary loop method; nonlinear system; linearization; parametric uncertainties; external disturbances; cross reactions.

I. INTRODUCTION

As is apparent from practice, it is important to research control algorithms functioning in order to avoid complications with their applications in real tasks. When these control techniques are designed for complex, expensive plants, for a wide class of similar systems or for novations in technologies, then laboratory platforms are usually used for their approbation.

A laboratory platform «Twin Rotor MIMO System» (TRMS) is designed for testing of control methods mainly for copters with different configurations. In simulations and design of control systems using this platform, it is required to take into account influence of measurement noises, resolution ability of sensors, hardware constraint of actuators control signals, parametrical uncertainties and external disturbances generated by vibrations, turbulences and so on.

Nowadays there are many results in identification and modeling of TRMS control using different approaches. Approaches based on adaptive and robust control methods are proposed in [1] – [6]. In [1] proportional-integral-derivative (PID) robust deadbeat control system based on the approach proposed in [7] was applied for a TRMS. The same idea was

Plant model analysis in sections II, III was financially supported by Government of Russian Federation, Grant 074-U01. Synthesis of control system in section V was supported by the Ministry of Education and Science of Russian Federation (Project 14.Z50.31.0031). Formulation of the Theorem in section V was supported by the Russian Federation President Grant (No. 14. W01.16.6325-MD (No. MD-6325.2016.8)). Control system approbation on laboratory platform was supported by the Russian Federation President Grant №14.Y31.16.9281-HIII.

implemented by authors of [2] in the designing of the time optimal robust control system. The robust adaptive fuzzy controller that uses gradient descent algorithm in order to increase plant robustness against external disturbances was presented in [3]. The sliding mode robust control method was implemented in [4]. Two different sliding mode controllers were combined into the robust control system designed for a cascade connected uncertain nonlinear systems and then applied for a TRMS in [5]. A robust model predictive control algorithm based on polytopic model representation was presented in [6].

A set of works propose optimal and suboptimal control techniques for a TRMS [8] – [13]. The LQR was implemented for TRMS control in [11], [12]. An optimal controller with iterative updating of a controller gain was presented in [9]. LQR with added integral action was designed in [10]. In [8] the fuzzy LQR based on Takagi–Sugeno fuzzy modeling technique [14] was designed. Particle swarm optimization technique was used in [13].

The current result is based on work [15] where the combination of optimal control algorithm and robust method of disturbances compensation proposed in [16] was applied to a linear system. Its effectiveness was illustrated by the academic example. In this paper, the same control technique is applied to a linearized model of TRMS and implemented to the laboratory platform. The proposed approach is considerate of both desired quality criteria and required robustness to undesired influences of parametric uncertainties and external disturbances. Presented experimental results are confirmation of that.

II. MODEL DESCRIPTION

Twin Rotor MIMO System laboratory platform is a helicopter-like nonlinear system with strong cross reactions and independent control for each degree of freedom. General view of TRMS is presented in Fig.1.

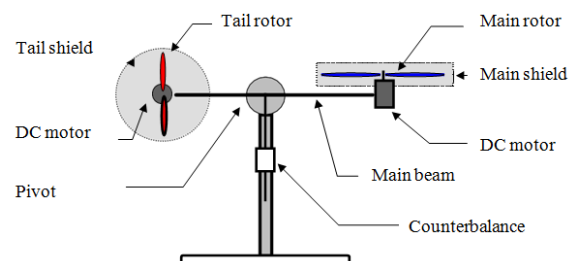


Fig. 1. Twin Rotor MIMO System

There are two known basic mathematical models of TRMS [17], [18]. They differ in dynamic equations and parameters. Most of the papers dealing with TRMS are usually based on one of them. For example, in [4] authors use model proposed in [17]. In [6] TRMS is analyzed with respect to model given in [18]. In [19] mean square error between the theoretical and experimental system trajectories is calculated for the case of model form documentation [18] and high quality of proposed description is shown. In this paper the model proposed in [18] is chosen with some additions from the documentation [17] analysis. These additions have no affect on the control system synthesis process and quality but they allow getting a more detailed description of the TRMS model.

For the purpose of simplification of controller synthesis and its attenuation, the TRMS is decomposed as two dynamically related subsystems such that each of them describes the plant dynamics in its own plane. Full dynamical model of the plant is presented by following equations

$$J_1 \ddot{\alpha} = -k_{f11} \dot{\alpha} - k_{f21} \text{sign}(\dot{\alpha}) + g(M - N) \cos \alpha - gP \sin \alpha - (M + N + P)\beta^2 \sin \alpha \cos \alpha + a_1 \tau_1 + b_1 \tau_1^2, \quad (1)$$

$$J_2 \ddot{\beta} = -k_{f21} \dot{\beta} - k_{f22} \text{sign}(\dot{\beta}) + \xi(\alpha, \dot{\alpha}, \ddot{\alpha}, t) + a_2 \tau_2 + b_2 \tau_2^2, \quad (2)$$

where $\alpha \in (-\pi/2; \pi/2)$ is a plant rotation angle in the vertical plane; $\beta \in (-3\pi/4; 3\pi/4)$ is rotation angle in the horizontal plane; J_1 is an inertia moment of the plant in vertical plane; $J_2 = S + T \sin^2 \alpha$ is an inertia moment in horizontal plane; $k_{f1i}, i = 1, 2$ are internal friction coefficients; $k_{f2i}, i = 1, 2$ are threshold friction coefficients; $g = 9.8 [m/s^2]$ is the acceleration of the free fall; $\tau_i, i = 1, 2$ are torque moments of DC motors; $a_i, b_i, i = 1, 2$ are DC motors static characteristic parameters; values of coefficients M, N, P, S, T satisfy following conditions:

$$\begin{aligned} M &= \left(\frac{m_t}{2} + m_{tr} + m_{ts}\right) l_t, \quad N = \left(\frac{m_m}{2} + m_{tr} + m_{ts}\right) l_m, \\ P &= \frac{m_b}{2} l_b + m_{cb} l_{cb}, \\ S &= \left(\frac{m_b}{3} l_b^2 + m_{cb} l_{cb}^2\right) + \left(m_{ms} r_{ms}^2 + \frac{m_{ts}}{2} r_{ts}^2\right), \\ T &= \left(\frac{m_m}{3} + m_{mr} + m_{ms}\right) l_m^2 + \\ &+ \left(\frac{m_t}{3} + m_{tr} + m_{ts}\right) l_t^2 - \left(\frac{m_b}{3} l_b^2 + m_{cb} l_{cb}^2\right), \end{aligned}$$

where m_t is tail beam mass, m_{tr} is tail DC motor and tail rotor mass, m_{ts} is tail shield mass, l_t is tail beam length, m_m is main beam mass, m_{tr} is tail DC motor and tail rotor mass, l_m is main beam length, m_b is counterbalance beam mass, l_b is counterbalance beam length, m_{cb} is counterbalance mass, l_{cb} is length between the counterbalance and the pivot, m_{ms} is main shield mass, r_{ms} is main shield radius, r_{ts} is tail shield radius, m_{mr} is main DC motor and main rotor mass.

Equation (1) describes the plant dynamic in the vertical plane and equation (2) does the same for the horizontal plane. Numerical values of plant parameters are in accordance with documentation [18] and shown in Table 1. Some of them were experimentally recalculated for the version of the platform used in experiments.

TABLE I. TWIN ROTOR MIMO SYSTEM PARAMETERS

Parameter	Value	Parameter	Value
m_{mr}	0.228 [kg]	r_{ms}	0.155 [m]
m_m	0.0145 [kg]	r_{ts}	0.1 [m]
m_{tr}	0.206 [kg]	J_1	0.0558 [kg*m ²]
m_t	0.0155 [kg]	k_{f11}	0.055 [n/a]
m_{cb}	0.068 [kg]	k_{f21}	0.001 [n/a]
m_b	0.022 [kg]	k_{f12}	0.095 [n/a]
m_{ms}	0.225 [kg]	k_{f22}	0.01 [n/a]
m_{ts}	0.165 [kg]	a_1	0.0135 [n/a]
l_m	0.24 [m]	a_2	0.02 [n/a]
l_t	0.25 [m]	b_1	0.0924 [n/a]
l_b	0.26 [m]	b_2	0.09 [n/a]
l_{cb}	0.13 [m]		

Remark. According to the documentation of TRMS [17], the control signal τ_i in (1) and (2) has the following form:

$$\tau_i = \frac{k_i}{T_{i1}s + T_{i0}} u_i, i = 1, 2,$$

where u_i is a voltage level on DC motor terminals. In this work simplification $\tau_i = u_i, i = 1, 2$ was used due to the fact that it is not clear how the numerical values of given transfer function coefficients were received. Moreover, in documentation [18] principally different model of the DC motor dynamics was given which has more information about the processes in TRMS actuators but much less formalized.

III. MODEL ANALYSIS

Model (1) in the state space representation can be written as:

$$\begin{cases} \dot{x}_{11} = y_1, \\ \dot{x}_{12} = \dot{x}_{11}, \\ \dot{x}_{12} = -\frac{k_{f11}}{J_1} x_{12} - \frac{k_{f12}}{J_1} \text{sign}(x_{12}) + \frac{g(M-N)}{J_1} \cos x_{11} - \\ - \frac{gP}{J_1} \sin x_{11} - \frac{M+N+P}{J_1} x_{21}^2 \sin x_{11} \cos x_{11} + \\ + \frac{a_1}{J_1} u_1 + \frac{b_1}{J_1} u_1^2, \end{cases} \quad (3)$$

where $y_1 = \alpha$. Model (2) in the state space representation is as follows:

$$\begin{cases} \dot{x}_{21} = y_2, \\ \dot{x}_{22} = \dot{x}_{21} = \dot{\beta}, \\ \dot{x}_{22} = -\frac{k_{f21}}{S+T \sin^2 x_{11}} x_{22} - \frac{k_{f22}}{S+T \sin^2 x_{11}} \text{sign}(x_{22}) + \\ + \frac{a_2}{S+T \sin^2 x_{11}} u_2 + \frac{b_2}{S+T \sin^2 x_{11}} u_2^2 + \xi(x_{11}, \dot{x}_{11}, \ddot{x}_{11}, t), \end{cases} \quad (4)$$

where $y_2 = \beta$. To simplify notation, the equations (3) and (4) are converted into the following form:

$$\begin{cases} \dot{x}_i = A_i x_i + B_i u_i + D f_i(t), \\ y_i = L_i x_i, \quad x_i(0) = x_{0i}, \quad i = 1, 2, \end{cases} \quad (5)$$

where $x_i = [x_{i1}, x_{i2}]^T$ is state vector; x_{0i} is initial condition; y_i, u_i are scalar output and input variables; $f_i(t)$ is function of

unknown disturbances caused by parametric uncertainty and unaccounted nonlinear dynamics; $A_i \in \mathbb{R}^{2 \times 2}$, $B_i \in \mathbb{R}^{2 \times 1}$, $D \in \mathbb{R}^{2 \times 1}$ are matrices with coefficients that may be unknown; L is an output matrix with known coefficients.

State, input and output matrices and input matrix for disturbances for subsystems (1) and (2) are as follows:

$$A_1 = \begin{bmatrix} 0 & 1 \\ \frac{g(M-N)}{J_1}(0.5 + \gamma_1) - \frac{gP}{J_1}(0.5 + \gamma_2) & -\frac{k_{f11}}{J_1} \end{bmatrix},$$

$$B_1 = \begin{bmatrix} 0 \\ \frac{b_1}{J_1} \end{bmatrix}, L = [1 \quad 0], D = \begin{bmatrix} 0 \\ 1 \end{bmatrix},$$

$$A_2 = \begin{bmatrix} 0 & 1 \\ 0 & -\frac{2k_{f21}}{2S+T} - \varphi_1 \end{bmatrix}, B_2 = \begin{bmatrix} 0 \\ -\frac{2a_2}{2S+T} - \varphi_2 \end{bmatrix},$$

where γ_i and φ_i , $i = 1, 2$ are interval additions that are originated from usage of the trigonometric function linearization techniques with regard to the working range of the plant [20]:

$$\sin x_{11} = \frac{\sin x_{11}}{x_{11}} x_{11} = [0; 1]x_{11} = 0.5x_{11} + [-0.5; 0.5]x_{11} = 0.5x_{11} + \gamma_1, \forall x_{11} \in (-\pi/2; \pi/2),$$

$$\cos x_{11} = \sin(x_{11} + \pi/2) = \frac{1}{2}(x_{11} + \pi/2) + [-0.5; 0.5](x_{11} + \pi/2) = \frac{1}{2}x_{11} + \gamma_2, \forall x_{11} \in (-\pi/2; \pi/2),$$

$$\sin^2 x_{11} = [0; 1], \forall x_{11} \in (-\infty; \infty).$$

Coefficients φ_1 and φ_2 were received by substituting the last expression into the third equation of system (4).

Disturbance functions take following forms:

$$f_1(x, t) = [0; 1]g(M - N)\frac{\pi}{2} - \frac{k_{f12}}{J_1}\text{sign}(x_{12}) + \frac{b_1}{J_1}u_1^2 - \frac{M+N+P}{J_1}\beta^2 \sin x_{11} \cos x_{11},$$

$$f_2(x, t) = -\frac{k_{f22}}{J_2}\text{sign}(x_{22}) + \xi(\alpha, \dot{\alpha}, \ddot{\alpha}, t) + \frac{b_2}{J_2}u_2^2.$$

In general, coefficients in matrices A_i, B_i and in $f_i(t)$, $i = 1, 2$ can vary over time or slightly differ from specified in manual.

IV. CONTROL PROBLEM STATEMENT

The following assumptions are made for the plant (5):

Assumptions:

1) The initial conditions x_{0i} , $i = 1, 2$ and dimensions n and m of plant matrices are known, $m < n$.

2) Conditions of structural compatibility are fulfilled:

$$\begin{cases} A_i = A_{mi} + B_{mi}c_{01i}^T, \\ B_i = B_{mi} + B_{mi}c_{02i}, i = 1, 2, \end{cases} \quad (6)$$

where $A_{mi} \in \mathbb{R}^{2 \times 2}$ is Hurwitz and $B_{mi} = [0 \quad b_{m2i}]$, $b_{m2i} \neq 0$ are known linear static matrices; c_{01i}^T is vector of unknown functions or constants and c_{02i} is unknown scalar that belong to the known bounded set Ξ .

3) Disturbances are unknown bounded functions.

4) Only output signals y_i and input control signals u_i , $i = 1, 2$ are available for measurement.

The stabilization task is chosen as a control goal:

$$|y_i| < \delta_i, t > t_{fi}, i = 1, 2, \quad (7)$$

where δ_i is a prespecified accuracy defined by technical requirements of the system, t_{fi} is a transient time.

Also, a suboptimal control task is considered which consists in the minimization of the following quality functional:

$$J_i = \int_0^\infty (y_i^T Q_i y_i + u_{oi}^T R_i u_{oi}) dt, i = 1, 2, \quad (8)$$

where $Q_i \geq 0$ is a weight matrix that influences the bound on the mean square error; $R_i > 0$ is a weight matrix that influences the control energy and thus it provides a control signal limitation.

V. SOLUTION METHOD

Parameterization of the model.

System (5) can be rewritten according to the condition of structural compatibility (6) in the following form:

$$\begin{cases} \dot{x}_i(t) = A_{mi}x_i(t) + B_{mi}c_{01i}^T x_i(t) + B_{mi}u_i(t) + \\ + B_{mi}c_{02i}u_i(t) + Df_i(t), \\ y_i(t) = Lx_i(t), i = 1, 2. \end{cases}$$

Let us group all addends that contain parametric uncertainties and unknown disturbances into the separate function:

$$\begin{cases} \dot{x}_i(t) = A_{mi}x_i(t) + B_{mi}u_i(t) + B_{mi}\psi_i(t), \\ y_i(t) = Lx_i(t), i = 1, 2, \end{cases} \quad (9)$$

where $\psi_i(t) = c_{01i}^T x_i(t) + c_{02i}u_i(t) + b_{m2i}^{-1}f_i(t)$ is a new function of uncertain influences.

Control law form.

Taking into account results [15] and [16], the control law for the system (9) is written in the following form:

$$u_i = u_{oi} + u_{ri}, i = 1, 2, \quad (10)$$

where u_{oi} is an optimal control law for the nominal part of the system that is responsible for the solution of the optimal stabilization task [21]; u_{ri} is a robust control law [16] that is necessary for the compensation of disturbances.

Taking (10) into account, the system (9) is rewritten as:

$$\begin{cases} \dot{x}_i(t) = A_{mi}x_i(t) + B_{mi}u_{oi}(t) + B_{mi}u_{ri}(t) + B_{mi}\psi_i(t), \\ y_i(t) = Lx_i(t), i = 1, 2. \end{cases} \quad (11)$$

Optimal control.

If $\psi_i(t) \equiv 0$, then $u_{ri} \triangleq 0$ and (11) can be rewritten as:

$$\begin{cases} \dot{x}_i(t) = A_{mi}x_i(t) + B_{mi}u_{oi}(t), \\ y_i(t) = Lx_i(t), i = 1, 2. \end{cases} \quad (12)$$

An optimal control law calculation is based on the algebraic Riccati equation [21]:

$$Q_i - K_i B_{mi} R_i^{-1} B_{mi}^T K_i + 2K_i A_{mi} = 0, i = 1, 2, \quad (13)$$

solved for the system (12) and in accordance with quality functional (8).

Solution of the equation (13) with respect to the matrix K_i and introduction of denotation $G_i = R_i^{-1} B_{mi}^T K_i$ yields the following optimal control law:

$$u_{oi}(t) = -G_i x_i(t), \quad i = 1, 2. \quad (14)$$

State vectors $x_i(t)$ are unmeasured but pairs (A_i, L) are observable so the control law (14) is rewritten as follows:

$$u_{oi}(t) = -G_i \hat{x}_i(t), \quad i = 1, 2, \quad (15)$$

where $\hat{x}_i(t)$ is estimation of the state vector $x_i(t)$ calculated by means of the observer:

$$\hat{\dot{x}}_{1i} = \frac{x_{1i}(t) - x_{1i}(t-\tau)}{\tau}, \quad \hat{\dot{x}}_{2i} = \frac{\hat{x}_{2i}(t) - \hat{x}_{2i}(t-\tau)}{\tau}, \quad i = 1, 2, \quad (16)$$

where τ is a delay value that is equal to the time sampling interval of the plant sensors.

Let us substitute control law (15) into the system (12):

$$\begin{cases} \dot{\hat{x}}_i(t) = A_{oi} \hat{x}_i(t), \\ \hat{y}_i(t) = L x_i(t), \quad i = 1, 2. \end{cases} \quad (17)$$

where $A_{oi} = A_{mi} - B_{mi} G_i$. The closed-loop system (17) has the optimal functioning in the sense of minimization of functional (8) in case if all disturbances are equal to zero. It is valid to say that system (17) describes the desired dynamics of the plant (11).

Robust control.

For the synthesis of the robust control in accordance with method [16] an auxiliary loop based on the model (17) is introduced in the following form:

$$\begin{cases} \dot{\hat{x}}_{ai}(t) = A_{oi} \hat{x}_{ai}(t) + B_{mi} u_{ri}(t), \\ \hat{y}_{ai}(t) = L x_{ai}(t), \quad i = 1, 2. \end{cases} \quad (18)$$

The mismatch error is considered:

$$\zeta_i(t) = x_i(t) - x_{ai}(t), \quad i = 1, 2. \quad (19)$$

Then, derivative of (19) is calculated as follows:

$$\begin{aligned} \dot{\zeta}_i &= A_{oi} x_i(t) + B_{mi} u_{ki}(t) + B_{mi} \psi_i(t) - \\ &\quad - A_{oi} x_{ai} - B_{mi} u_{ki}, \quad i = 1, 2. \\ \dot{\zeta}_i &= A_{oi} \zeta_i(t) + B_{mi} \psi_i(t), \quad i = 1, 2. \end{aligned} \quad (20)$$

Let us choose in (20) a k -th row which corresponds to the non-zero element in the vector B_{mi} :

$$\dot{\zeta}_{ki} = A_{oki} \zeta_i(t) + B_{mki} \psi_i(t), \quad i = 1, 2. \quad (21)$$

Signal $\psi_i(t)$ can be expressed from the (21) as follows:

$$\psi_i(t) = B_{mki}^{-1} (\dot{\zeta}_{ki} - A_{oki} \zeta_i(t)), \quad i = 1, 2. \quad (22)$$

Substitution of (22) and (15) into (11) yields:

$$\begin{cases} \dot{\hat{x}}_i(t) = A_{oi} \hat{x}_i(t) + B_{mi} u_{ri}(t) + \\ + B_{mi} B_{mki}^{-1} (\dot{\zeta}_{ki} - A_{oki} \zeta_i(t)), \\ \hat{y}_i(t) = L x_i(t), \quad i = 1, 2. \end{cases} \quad (23)$$

The control law of the following form

$$u_{ri}(t) = -B_{mki}^{-1} (\dot{\zeta}_{ki} - A_{oki} \zeta_i(t)), \quad i = 1, 2, \quad (24)$$

compensates influence of $\psi_i(t)$ but vectors $\zeta_i(t)$ as well as derivatives $\dot{\zeta}_{ki}$ in (24) are unmeasured. Therefore, the real control law can be written as follows:

$$u_{ri}(t) = -B_{mki}^{-1} (\dot{\hat{\zeta}}_{ki} - A_{oki} \hat{\zeta}_i(t)), \quad i = 1, 2, \quad (25)$$

where $\hat{\zeta}_i(t)$ и $\dot{\hat{\zeta}}_{ki}$ are estimates of vectors $\zeta_i(t)$ and derivatives $\dot{\zeta}_{ki}$ respectively. Taking into account the fact that output mismatch errors $\zeta_{1i}(t) = x_1(t) - x_{a1}(t) = y - y_a$, $i = 1, 2$ are available for measurement, the estimates are calculated as

$$\hat{\zeta}_{1i} = \frac{\zeta_{1i}(t) - \zeta_{1i}(t-\tau)}{\tau}, \quad \dot{\hat{\zeta}}_{ji} = \frac{\hat{\zeta}_{ji}(t) - \hat{\zeta}_{ji}(t-\tau)}{\tau}, \quad j = 1, 2. \quad (26)$$

By substituting (15) and (25) into (10) the final form of control law is gained:

$$u_i(t) = -G_i \hat{x}_i(t) - B_{mki}^{-1} (\dot{\hat{\zeta}}_{ki} - A_{oki} \hat{\zeta}_i(t)), \quad i = 1, 2. \quad (27)$$

Theorem. Let assumptions hold. Then there exists parameter τ such that for $\tau \leq \tau_0$ the control algorithm for the plant (11) that consists of the control law (27), observers (16) and (26) and auxiliary loop (18) satisfies the control goal (7) and minimizes the quality functional (8).

The proof of the Theorem is equal to the proof in [15].

VI. SIMULATION RESULTS

In the practical experiment, the regulator is implemented via Simulink/MATLAB software on PC connected with the TRMS 33-220 platform. Regulator structure is synthesized in accordance with the algorithm presented in Section V with numerical parameters chosen as follows. Using Table 1 information, matrices of the nominal plant (12) are calculated as:

$$\begin{aligned} A_{m1} &= A_1|_{\gamma_1=0, \gamma_2=0} = \begin{bmatrix} 0 & 1 \\ -2.2491 & -0.9849 \end{bmatrix}; \\ B_{m1} &= B_1 = \begin{bmatrix} 0 \\ 1.6116 \end{bmatrix}; \quad A_{m2} = A_2|_{\varphi_1=0} = \begin{bmatrix} 0 & 1 \\ 0 & -1.5013 \end{bmatrix}; \\ B_{m2} &= B_2|_{\varphi_2=0} = \begin{bmatrix} 0 \\ 2.8446 \end{bmatrix}; \quad L = \begin{bmatrix} 1 & 0 \end{bmatrix}. \end{aligned}$$

As second row of B_{mi} , $i = 1, 2$ is non-zero, then in this case in (27) $k = 2$. Quality functional is defined in accordance with equation (8) with the following weight matrices: $Q_1 = 0.5$, $Q_2 = 0.001$, $R_1 = 0.6$, $R_2 = 1.9$. Optimal feedback matrices G_i are $G_1 = [0.2720 \quad 0.2321]$, $G_2 = [0.0229 \quad 0.0012]$. Auxiliary loop (18) state matrices A_{oi} are presented as follows:

$$A_{o1} = \begin{bmatrix} 0 & 1 \\ -2.6875 & -1.359 \end{bmatrix}, \quad A_{o2} = \begin{bmatrix} 0 & 1 \\ -0.0653 & -18.9675 \end{bmatrix}.$$

Estimates in (27) are calculated by observers (16) and (26) where parameter $\tau = 0.01$ s.

To suppress measurement noises the following filter was used:

$$y_{i_filtered} = \frac{1}{0.01p^2+p} y_{i_measured}, \quad p = \frac{d}{dt}, \quad i = 1, 2.$$

Experimental results are shown in Fig. 2.

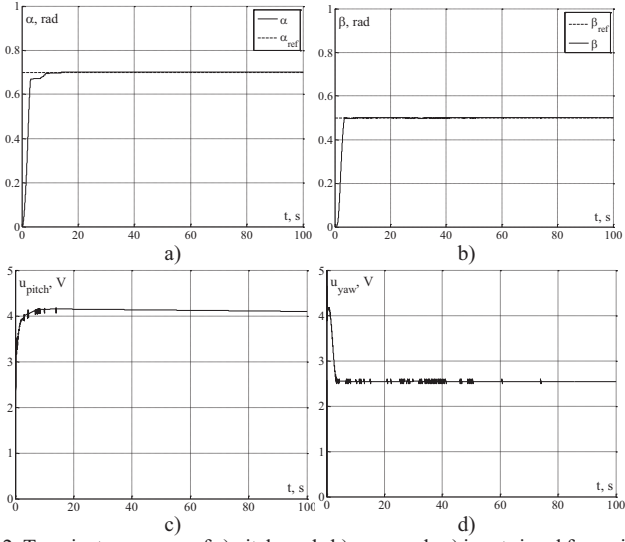


Fig. 2. Transient processes of a) pitch angle b) yaw angle c) input signal for main rotor d) input signal for tail rotor. Case of robust suboptimal algorithm.

Received data showed the following results of control application to the TRMS rig. Output error value in the steady state in both degrees of freedom did not exceed the resolution ability of encoders. Control signals did not saturate. Overshoot is absent. Precise values of transient time t_{fi} , overshoot σ_i and the set of attraction bounds $\delta_i, i = 1, 2$ are presented in Table 3. Deviations of integral quality criteria of the considered system from the same criteria for the simplified ideal model (12) are calculated as follows:

$$\Delta J_i = J_{i_real} - J_{i_ideal}, \quad (28)$$

$$\Delta J_{yi} = J_{yi_real} - J_{yi_ideal}, \quad (29)$$

$$\Delta J_{ui} = J_{ui_real} - J_{ui_ideal}, i = 1, 2, \quad (30)$$

In equations (28) – (30) J_i is an integral quality criteria calculated by equation (8); $J_{yi} = \int_0^\infty y_i^T Q_i y_i dt$, $J_{ui} = \int_0^\infty u_i^T Q_i u_i dt$, where index *real* (*ideal*) corresponds to the case of real (*ideal*) plant regulated by robust suboptimal (suboptimal) controller. Numerical values of these criteria for the control system considered in the experiment are presented in Table 2.

To demonstrate advantages of the proposed algorithm, its functioning is compared with the suboptimal control system with the regulator of the following form:

$$u_{oi}(t) = -G_i \hat{x}_i(t), i = 1, 2,$$

calculated using functional (8) where $Q_1 = 1$, $Q_2 = 1$, $R_1 = 0.35$, $R_2 = 0.055$. Different values of weight matrices are needed to achieve required quality of transfer responses. This fact does not allow to compare control systems by the integral quality criteria. Experimental results are shown in Fig. 3.

TABLE II. INTEGRAL QUALITY CRITERIA VALUES

Quality indicator	Degree of freedom	
	Pitch, $i = 1$	Yaw, $i = 2$
ΔJ_i , [n/a]	-1034.31	-408.4861
ΔJ_{yi} , [rad ²]	-22.341	-10.6524
ΔJ_{ui} , [V ²]	-1011.9682	-397.8337

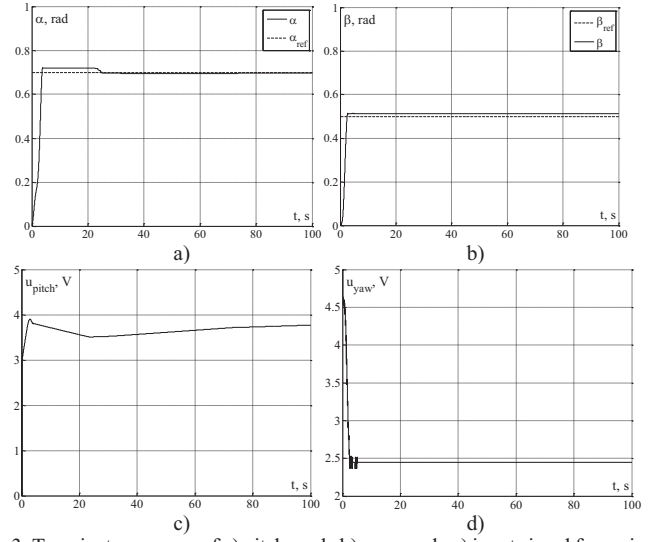


Fig. 3. Transient processes of a) pitch angle b) yaw angle c) input signal for main rotor d) input signal for tail rotor. Case of optimal algorithm.

In this case, experimental data showed the following results. Output error value in the steady state in both degrees of freedom is sufficiently small and did not exceed the 3% of the desired value. Control signals did not saturate. Small overshoot is present. Precise values of transient time t_{fi} , overshoot σ_i and the set of attraction bounds $\delta_i, i = 1, 2$ are presented in Table 3.

In addition, obtained results are compared with classical PID controller. Including the noises suppress filter led to the instability of the closed-loop system so the filter was excluded. Experimental results are shown in Fig. 4.

As can be seen from the received results, output error value in the steady state in both degrees of freedom is sufficiently small and did not exceed the 2% of the desired value. Control signals were saturated for the lack of the filter in control system structure and because of the influence of PID integral term. Considerable overshoot is present. Precise values of transient time t_{fi} , overshoot σ_i and the set of attraction bounds $\delta_i, i = 1, 2$ are presented in Table 3.

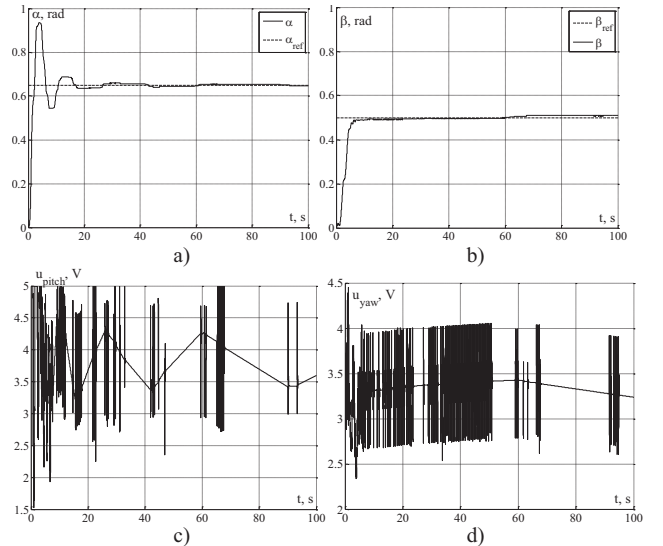


Fig. 4. Transient processes of a) pitch angle b) yaw angle c) input signal for main rotor d) input signal for tail rotor. Case of PID algorithm.

TABLE III. QUALITY INDICATORS

	Quality indicator	Control method		
		<i>Robust Suboptimal</i>	<i>Suboptimal</i>	<i>PID</i>
pitch	t_{f1} , [s]	8.5	4	16
	δ_1 , [%]	1	3	2
	σ_1 , [%]	0	3.6	43.8
yaw	t_{f2} , [s]	3.5	2.4	9.9
	δ_2 , [%]	0.6	2.4	2
	σ_2 , [%]	0	3.1	0

VII. CONCLUSION

The main contribution of this work is in the application of the robust suboptimal algorithm [15] to the control of the Twin Rotor MIMO System test rig. The goal of this research was twofold: to analyze the control method functioning in the practical case and to research advantages of the chosen algorithm for the solution of the TRMS control problem and consequently copters control task.

Received experimental results allowed to draw following conclusions. It is demonstrated that the control algorithm can be applied to the task of nonlinear Lipchitz systems control with compensation of most kinds of disturbances. Comparing with similar algorithms (PID and suboptimal controllers), experiments showed that proposed control method achieves considerably better accuracy in steady state. Due to the size limitations of this paper, it was not possible to show here simulation comparison with more control approaches. Based on the experimental data in similar papers the following assumptions about the quality advantages of the proposed algorithm can be made. For example, in [4] transients of angles have large amplitudes of fluctuations and transient time is longer than in current work. Also proposed approach has better transient time than in [5] as well as in all approaches with which its author compares his results.

ACKNOWLEDGMENT

Great thanks to our colleague Nina A. Vunder for her expert advice on usage of interval linearization methods.

REFERENCES

- [1] Wen, Peng, and T-W. Lu. "Decoupling control of a twin rotor MIMO system using robust deadbeat control technique." IET Control Theory & Applications 2.11 (2008): 999-1007.
- [2] Lu, Te-Wei, and Peng Wen. "Time optimal and robust control of twin rotor system." 2007 IEEE International Conference on Control and Automation. IEEE, 2007.
- [3] Jahed, Maryam, and Mohammad Farrokhi. "Robust adaptive fuzzy control of twin rotor MIMO system." Soft Computing 17.10 (2013): 1847-1860.

- [4] Huang, Loulin. "An approach for robust control of a twin-rotor multiple input multiple output system." Robotics and Automation (ICRA), 2011 IEEE International Conference on. IEEE, 2011.
- [5] Su, Juhng-Peng, Chi-Ying Liang, and Hung-Ming Chen. "Robust control of a class of nonlinear systems and its application to a twin rotor MIMO system." Industrial Technology, 2002. IEEE ICIT'02. 2002 IEEE International Conference on. Vol. 2. IEEE, 2002.
- [6] Rahideh, Akbar, and M. Hasan Shaheed. "Robust model predictive control of a twin rotor MIMO system." Mechatronics, 2009. ICM 2009. IEEE International Conference on. IEEE, 2009.
- [7] Dawes, J., et al. "Design of deadbeat robust systems." Control Applications, 1994., Proceedings of the Third IEEE Conference on. IEEE, 1994.
- [8] Tao, Chin-Wang, Jin-Shiuh Taur, and Y. C. Chen. "Design of a parallel distributed fuzzy LQR controller for the twin rotor multi-input multi-output system." Fuzzy Sets and Systems 161.15 (2010): 2081-2103.
- [9] Pratap, Bhanu, Abhishek Agrawal, and Shubhi Purwar. "Optimal control of twin rotor MIMO system using output feedback." Power, Control and Embedded Systems (ICPES), 2012 2nd International Conference on. IEEE, 2012.
- [10] Phillips, Andrew, and Ferat Sahin. "Optimal control of a twin rotor mimo system using lqr with integral action." 2014 World Automation Congress (WAC). IEEE, 2014.
- [11] Pandey, Sumit Kumar, and Vijaya Laxmi. "Optimal Control of Twin Rotor MIMO System Using LQR Technique." Computational Intelligence in Data Mining-Volume 1. Springer India, 2015. 11-21.
- [12] Ahmad, S. M., A. J. Chipperfield, and O. Tokhi. "Dynamic modeling and optimal control of a twin rotor MIMO system." National Aerospace and Electronics Conference, 2000. NAECON 2000. Proceedings of the IEEE 2000. IEEE, 2000.
- [13] Allouani, F., D. Boukhetala, and F. Boudjema. "Particle swarm optimization based fuzzy sliding mode controller for the twin rotor MIMO system." 2012 16th IEEE Mediterranean Electrotechnical Conference. IEEE, 2012.
- [14] Takagi, Tomohiro, and Michio Sugeno. "Fuzzy identification of systems and its applications to modeling and control." IEEE transactions on systems, man, and cybernetics 1 (1985): 116-132.
- [15] Furtat, Igor B. "Robust suboptimal control with disturbances compensation." 2014 19th International Conference on Methods and Models in Automation and Robotics (MMAR). 2014.
- [16] Tsykunov, Aleksandr M. "Robust control algorithms with compensation of bounded perturbations." Automation and Remote Control 68.7 (2007): 1213-1224.
- [17] Twin Rotor M. System Control Experiments 33-949S, Feedback Instruments Ltd //East Sussex, UK. – 2006.
- [18] Twin Rotor M. System Advanced Teaching Manual 1 (33-007-4M5) //Feedback Instruments Ltd, Crowborough, UK. – 1998.
- [19] Rahideh, A., M. H. Shaheed, and H. J. C. Huijberts. "Dynamic modelling of a TRMS using analytical and empirical approaches." Control Engineering Practice 16.3 (2008): 241-259.
- [20] Akunov, T. A.; Akunova, A.; Ushakov, A. V. "Fuzzy identification of systems and its applications to modeling and control." Proceedings of 5th IFAC Symposium on Nonlinear Control Systems. VOLS 1-3, 837-842 – 2001.
- [21] M. A. Athans and P. L. Falb. Optimal Control. New York: McGraw-Hill, 1966.